Journal of Cerebral Blood Flow & Metabolism (2006) 26, 1198–1212

www.jcbfm.com

Positron emission tomography of monoaminergic vesicular binding in aging and Parkinson disease

Nicolaas I Bohnen[1], Roger L Albin[2,3], Robert A Koeppe[1], Kristine A Wernette[1,2], Michael R Kilbourn[1], Satoshi Minoshima[1,4] and Kirk A Frey[1,2]

[1]*Department of Radiology (Division of Nuclear Medicine), The University of Michigan Medical School, Ann Arbor, Michigan, USA;* [2]*Department of Neurology, The University of Michigan Medical School, Ann Arbor, Michigan, USA;* [3]*Geriatric Research, Education and Clinical Center, Veterans Affairs Medical Center, Ann Arbor, Michigan, USA*

The type-2 vesicular monoamine transporter (VMAT2) might serve as an objective biomarker of Parkinson disease (PD) severity. Thirty-one subjects with early-stage PD and 75 normal subjects underwent continuous intravenous infusion of (+)-[^{11}C]dihydrotetrabenazine (DTBZ) and positron emission tomography (PET) imaging to estimate the striatal VMAT2 binding site density with equilibrium tracer modeling. Parkinson disease patients were evaluated clinically in the practically defined 'off' state with the Unified Parkinson Disease Rating Scale (UPDRS), the Hoehn and Yahr Scale (HY), and the Schwab and England Activities of Daily Living Scale (SE). In normal subjects there was age-related decline in striatal DTBZ binding, approximating 0.5% per year. In PD subjects, specific DTBZ binding was reduced in the caudate nucleus (CD; −44%), anterior putamen (−68%), and posterior putamen (PP; −77%). The PP-to-CD ratio of binding was reduced significantly in PD subjects. Dihydrotetrabenazine binding was also reduced by approximately 50% in the PD substantia nigra. Striatal binding reductions correlated significantly with PD duration and SE scores, but not with HY stage or with UPDRS motor subscale ($UPDRS_{III}$) scores. Striatal and midbrain DTBZ binding was asymmetric in PD subjects, with greatest reductions contralateral to the most clinically affected limbs. There was significant correlation between asymmetry of DTBZ binding and clinical asymmetry measured with the $UPDRS_{III}$. In HY stage 1 and 1.5 subjects ($n=16$), PP DTBZ binding contralateral to the clinically unaffected body side was reduced by 73%, indicating substantial preclinical nigrostriatal pathology in PD. We conclude that (+)-[^{11}C]DTBZ-PET imaging displays many properties necessary of a PD biomarker.
Journal of Cerebral Blood Flow & Metabolism (2006) **26,** 1198–1212. doi:10.1038/sj.jcbfm.9600276; published online 18 January 2006

Keywords: positron emission tomography; VMAT2; Parkinson disease; aging; striatum

Introduction

Development of a robust, objective marker of Parkinson disease (PD) severity would improve significantly our understanding of disease progression, and would assist evaluation of potential neuroprotective therapies (Brooks *et al*, 2003). Several radiotracers have been employed to image nigrostriatal terminals *in vivo*, including [^{18}F]fluorodopa (FDOPA; Garnett *et al*, 1983), which measures aromatic amino-acid decarboxylase (AADC) activity, and plasmalemmal dopamine transporter (DAT) ligands, such as [^{11}C]nomifensine (Leenders *et al*, 1990*b*) and various cocaine analogs (Frost *et al*, 1993; Seibyl *et al*, 1995). *In vivo* human use of FDOPA or DAT ligands in PD and other disorders characterized by loss of nigrostriatal neurons has documented substantial loss of these nigrostriatal dopamine terminal markers. Individual tracer and imaging methods, however, give differing quantitative estimates of abnormality in PD. *In vivo* DAT imaging studies, for example, show severe reductions in PD striatum (Leenders *et al*, 1990*b*; Frost *et al*, 1993; Seibyl *et al*, 1995), corresponding to postmortem findings of markedly reduced putaminal DAT protein (Niznik *et al*, 1991; Kaufman and Madras, 1991; Chinaglia *et al*, 1992). [^{18}F]6-fluoro-

Correspondence: Dr KA Frey, Division of Nuclear Medicine, Department of Radiology, The University of Michigan, Room B1 G505 University Hospital, 1500 East Medical Center Drive, Ann Arbor, MI 48109-0028, USA.
E-mail: kfrey@umich.edu
[4]Current address: Department of Radiology, University of Washington, Seattle, WA, USA.
This study was supported in part by NS15655 from the National Institutes of Health, and a VA Merit Review award.
Received 29 April 2005; revised 9 December 2005; accepted 13 December 2005; published online 18 January 2006

dopa studies suggest more modest nigrostriatal losses in PD (Eidelberg *et al*, 1990; Sawle *et al*, 1994; Antonini *et al*, 1995; Ishikawa *et al*, 1996; Morrish *et al*, 1996*b*). These apparent differences might be explained by a number of factors, including studying subjects at different clinical stages, differences in tracer specificity and differences in imaging technology. Perhaps most important is the possibility of differential regulation of tracer target proteins by compensation for partial losses of dopaminergic nerve terminals and in response to dopaminergic drug treatments. Considerable preclinical and some human evidence indicate that AADC activity and cell surface DAT expression are each regulated by dopamine receptor activation and changes in synaptic DA levels (Weiner *et al*, 1989; Hadjiconstantinou *et al*, 1993; Young *et al*, 1993; Zhu *et al*, 1993, 1997; Meiergerd *et al*, 1994; Wilson *et al*, 1994, 1996*b*; Cumming *et al*, 1995; Vander Borght *et al*, 1995*b*; Reith *et al*, 1997; Pristupa *et al*, 1998; Tedroff *et al*, 1999; Daniels and Amara, 1999; Melikian and Buckley, 1999; Lee *et al*, 2000; Guttman *et al*, 2001; Doolen and Zahniser, 2001). Aromatic amino-acid decarboxylase activity might be upregulated and DAT expression on the cell surface membrane might be downregulated in the partially dopamine denervated striatum. Potential difficulties with use of FDOPA and DAT ligands for quantification of nigrostriatal terminal density in recent neuroprotection/neurotoxicity studies of dopamine agonists (CALM-PD-Parkinson Study Group, 2002; REAL-PET; Whone *et al*, 2003) and levodopa (ELLDOPA-Parkinson Study Group, 2004) are highlighted by controversy over the interpretation of imaging data (Albin *et al*, 2002; Ahlskog, 2003; Albin and Frey, 2003). In the CALM-PD and ELLDOPA trials, the results of DAT imaging studies were discordant with the results of clinical measures of PD progression.

An alternative target for quantitative imaging of nigrostriatal terminals is the type-2 vesicular monoamine transporter (VMAT2; Frey *et al*, 1996*a*; Kilbourn, 1997), the protein responsible for translocating monoamine neurotransmitters from the cytoplasm into synaptic vesicles. In the CNS, VMAT2 is expressed exclusively by monoaminergic—dopaminergic, serotonergic, norepinephrinergic, or histaminergic—neurons (Scherman *et al*, 1988; Erickson and Eiden, 1993). Over 95% of striatal VMAT2 binding sites are associated with dopaminergic terminals (Vander Borght *et al*, 1995*a*; Wilson *et al*, 1996*b*) and striatal VMAT2 binding site density is a linear function of mesencephalic nigrostriatal neuron number (Vander Borght *et al*, 1995*a*). Type-2 vesicular monoamine transporter binding is predicted to be unaffected by dopaminergic agents or synaptic dopamine levels because synaptic vesicle function is apparently regulated by transfer of vesicles between reserve and actively cycling synaptic terminal pools with relatively stable vesicle numbers (Greengard *et al*, 1993). Experimental evidence is consistent with this prediction; VMAT2 binding is not affected by dopaminergic drug treatments that cause changes in dopamine receptor or DAT expression (Naudon *et al*, 1994; Vander Borght *et al*, 1995b; Kilbourn *et al*, 1996; Wilson and Kish, 1996*a*; Kemmerer *et al*, 2003).

Previously, we showed the successful *in vivo* human imaging of striatal VMAT2 with [^{11}C]dihydrotetrabenazine (DTBZ) and positron emission tomography (PET) (DTBZ-PET; Frey *et al*, 1996*a*). We and others showed reduced striatal DTBZ binding in PD, multiple system atrophy, REM sleep behavior disorder, and normal aging (Frey *et al*, 1996*a*; Gilman *et al*, 1996; Albin *et al*, 2000; Lee *et al*, 2000). Our prior study of PD reported results from relatively small subject groups (7 PD; 15 normal subjects) and employed the racemic ligand (±)-[^{11}C]DTBZ. As only the (+) enantiomer binds specifically to VMAT2, use of the racemic tracer degrades specificity and reduces image contrast. Subsequent resolution of DTBZ enantiomers allowed development of the more specific tracer (+)-[^{11}C]DTBZ (Kilbourn *et al*, 1995).

In the present studies, we extend our VMAT2 imaging experience employing (+)-[^{11}C]DTBZ in relatively large numbers of normal and PD subjects. We evaluate the possible loss of striatal VMAT2 binding in normal aging and assess the pattern of reduced VMAT2 binding in PD. We further investigate the relationships of VMAT2 binding losses to clinical measures of disease severity and asymmetry in patients with mild-to-moderate PD.

Patients and methods

Subjects

Thirty-one subjects with PD (20 men, 11 women; age 64 ± 10 years (mean ± s.d.)—range 43 to 89 years; Table 1) and 75 normal subjects (40 men, 35 women; age 49 ± 15 years—range 20 to 79 years) underwent PET imaging with (+)-[^{11}C]DTBZ. The duration of symptomatic PD was 5 ± 3 years (range 1 to 15 years) at the time of imaging. Parkinson disease diagnosis was based on conventional criteria requiring the presence of at least two cardinal signs (resting tremor, bradykinesia, rigidity) and responsiveness to levodopa and or dopamine agonist treatment. No subjects had atypical features such as prominent cognitive impairment or postural instability within the first year or had supranuclear eye movement abnormalities (Gelb *et al*, 1999). Three subjects were untreated for PD at the time of PET imaging, but later showed symptomatic treatment responses. Of the remaining subjects, 25 were receiving carbidopa-levodopa, 5 dopamine agonists, 9 selegiline, 2 trihexyphenidyl, and 1 tolcapone. Parkinson disease subjects were examined clinically in the practically defined 'off' state (12 h after the last medication dosages) using the Unified Parkinson Disease Rating Scale (UPDRS; Fahn and Elton, 1987), the modified Hoehn and Yahr Scale (HY; Hoehn and Yahr, 1967), and the Schwab and England (1969) Activities of

Table 1 Parkinson disease subject characteristics

Age	*Gender*	*Duration*	*HY*	*SE*	*UPDRS$_{III}$*	T	R	B	*Medications*[a]
43	M	3	1.0	0.9	6	+	+	+	L—240
44	F	5	1.0	1.0	4	+	+	+	L—400; D—10
53	F	5	1.0	0.9	8	+	+	+	L—300
57	M	4	1.0	0.9	16	+	+	+	L—300
58	M	1	1.0	0.9	8	+	+	+	L—400; D—10
63	F	3	1.0	1.0	10	+	–	+	D—5
67	M	2	1.0	0.8	17	+	+	+	None
71	F	1	1.0	1.0	10	+	+	+	None
48	F	1	1.5	0.8	9	+	+	+	P—3
59	M	7	1.5	0.9	16	–	+	+	L—100; P—6; D—5
61	M	1	1.5	0.9	8	+	+	+	None
64	M	3	1.5	0.9	9	+	-	+	P—1.5
68	M	2	1.5	0.8	10	+	+	+	L—600
73	M	8	1.5	0.9	7	+	+	+	L—480; D—5
74	M	7	1.5	0.8	10	+	+	+	L—1000; Br—22.5; D—10
80	M	3	1.5	0.9	7	–	+	+	L—500
54	M	8	2.0	0.8	23	+	+	+	L—580
60	M	12	2.0	0.8	27	+	+	+	L—980; D—5
64	M	6	2.0	0.8	27	+	+	+	L—960; Tr—8
68	F	8	2.0	0.9	10	+	+	+	L—750
68	F	4	2.0	0.8	13	+	+	+	L—300
75	F	5	2.0	0.8	13	+	+	+	L—420; D—5
76	M	22	2.0	1.0	20	–	+	+	L—400
58	M	5	2.5	0.8	26	+	+	+	L—140; Tr—8; D—5
60	M	3	2.5	0.9	23	+	+	+	L—300; To—600
63	M	5	2.5	0.8	19	+	+	+	L—630
64	F	10	2.5	0.8	40	+	+	+	L—560; Br—15; D—5
79	M	6	2.5	0.7	34	+	+	+	L—800
89	F	1	2.5	0.9	20	+	+	+	L—280
68	M	8	3.0	0.7	33	+	+	+	L—630; D—5
69	F	15	3.0	0.8	30	+	+	+	L—800

[a]Values reflect the total daily medication dosages. Sustained-release levodopa was scaled by 0.75, reflecting its incomplete bioavailability.
B = bradykinesia; Br = bromocriptine; D = deprenyl; L = levodopa; P = pergolide; R = rigidity; T = tremor; To = tolcapone; Tr = trihexyphenidyl.

Daily Living Scale (SE). Patients were allowed to resume medication after clinical ratings and before PET scans. All patients had mild-to-moderate PD (HY 1 to 3: stage 1: $n = 8$; stage 1.5: $n = 8$; stage 2: $n = 7$, stage 2.5: $n = 6$; and stage 3: $n = 2$ patients).

None of the normal subjects were taking psychotropic drugs or had a history of neurological, psychiatric, or major medical diseases, and all had a normal neurologic examination. The experimental protocol was approved by The University of Michigan committees on the use of human subjects in research and on the human use of radioisotopes, and written informed consent was obtained before all procedures.

(+)-[^{11}C]Dihydrotetrabenazine Positron Emission Tomography Scans

No-carrier-added (+)-[^{11}C]DTBZ (250 to 1000 Ci/mmol at the time of injection) was prepared as reported previously (Jewett *et al*, 1997). Positron emission tomography image data were acquired in three-dimensional mode (septa retracted) on a Siemens/CTI ECAT EXACT-47 scanner (Knoxville, TN, USA), which images a 15.8 cm axial field-of-view and permits reconstruction of 47 contiguous 3.375-mm-thick tissue slices. All subjects were studied supine, with eyes and ears unoccluded, resting quietly in a dimly lit room. Subjects were injected with 10 to 18 mCi (370 to 666 MBq) of (+)-[^{11}C]DTBZ containing less than 50 μg DTBZ mass. At this dosage, less than 10% of striatal VMAT2 binding sites could be occupied (less than 10 nmol/L [^{11}C]DTBZ peak striatal concentration and approximately 100 nmol/L striatal VMAT2 concentration as reported by Scherman *et al*, 1989). In all, 55% of the dose was administered by intravenous bolus injection over the first 15 to 30 secs of the study, while the remaining 45% of the dose was continuously infused over the next 60 mins, resulting in stable arterial tracer levels and equilibrium with brain tracer levels after 30 mins (Koeppe *et al*, 1997). A series of 4 PET image frames were acquired: 0 to 4 mins; 30 to 40 mins; 40 to 50 mins; and 50 to 60 mins. Each frame was reconstructed using a Hanning filter with a cutoff of 0.5 cycles/projection ray, achieving a reconstructed resolution of approximately 9 mm full-width at half-maximum. The measured attenuation correction was applied to all image frames based on a 10- to 12-min 2-D transmission scan performed immediately before DTBZ injection. Images were corrected for scattered events by the method of Ollinger and Johns (1993) and Ollinger (1995) as implemented by CTI, Inc. All image frames were spatially coregistered within subjects with a rigid-body transformation to reduce the effects of subject motion during the imaging session (Minoshima *et al*, 1993*b*), followed by linear transformation to a reference atlas anatomical

orientation (Talairach and Tournoux, 1988) and scale (Minoshima *et al*, 1993*a*, 1994).

Blood samples were withdrawn from a radial artery catheter at 10-sec intervals for the first 2 mins, and then at 2.5, 3, 4, 30, 40, 50, and 60 mins after DTBZ injection. Plasma was separated from red blood cells by centrifugation and was assayed for ^{11}C activity in a NaI well counter. Aliquots of plasma obtained at 1, 2, and 3 mins and thereafter were also processed for determination of radiolabeled metabolites using a rapid Sep-Pak C_{18} chromatographic technique (Frey *et al*, 1992). Plasma (0.5 mL) was added to phosphate-buffered saline (PBS, 0.5 mL) containing approximately 0.05 μCi of authentic [^{3}H]DTBZ and the sample was applied to a Sep-Pak C_{18} chromatography column. The eluates: (1) from initial column loading combined with a subsequent wash with 9 mL of PBS:ethanol, 65:35, and (2) from a subsequent wash with 5 mL of absolute ethanol, were each assayed for ^{11}C activity in the well counter. After decay of the ^{11}C, aliquots of the two eluates were assayed for tritium content by liquid scintillation spectrometry. The distribution of [^{3}H]DTBZ between the two eluates was used to correct for losses (approximately 20%) of unmetabolized (+)-[^{11}C]DTBZ eluted with the metabolites in the first column wash.

Parametric Dihydrotetrabenazine Transport and Type-2 Vesicular Monoamine Transporter Binding Maps

Equilibrium modeling was used to estimate the total tissue-to-plasma distribution volume (DV_{tot}) in each imaged voxel (Koeppe *et al*, 1997). The average concentration of (+)-[^{11}C]DTBZ in tissue measured with PET (C_{PET}) in the three 10-min duration images between 30 and 60 mins after beginning infusion of DTBZ was divided by the metabolite-corrected arterial plasma concentration (C_P) averaged over the 30-, 40-, 50-, and 60-min samples:

$$DV_{tot} = C_{PET}/C_P \quad (1)$$

DV_{tot} contains contributions of free and nonspecifically bound ligand (DV_{ns}) in addition to that of specifically bound ligand (DV_{sp}). Measured plasma and brain regional concentrations varied on average by 2% to 4% during the 30- to 60-min equilibrium period. We estimated specific DTBZ binding by subtraction of the occipital cortex value (DV_{ctx}), a reference region very low in VMAT2 binding sites, with the assumption that the free and nonspecific distribution is uniform across the brain ($DV_{ns} = DV_{ctx}$) at equilibrium:

$$DV_{sp} = DV_{tot} - DV_{ns} \quad (2)$$

Expression of DV_{sp} relative to DV_{ns} results in a binding potential (BP; Mintun *et al*, 1984; Lammertsma *et al*, 1996), which is proportional to the density of tissue-binding sites (B_{max}) divided by the equilibrium ligand dissociation constant (K_d):

$$BP = DV_{sp}/DV_{ns} \approx B_{max}/K_d \quad (3)$$

(the Lammertsma *et al* (1996) definition of BP). The assumption of minimal specific (+)-[^{11}C]DTBZ binding in the occipital cortex is supported by *in vitro* VMAT2 binding results in rodent and human brain, which indicate cortical binding levels between 5% and 8% of those in the caudate nucleus (CD) and putamen (Vander Borght *et al*, 1995*a*; Scherman *et al*, 1988) and by prior human PET imaging studies comparing the distributions of the active (+)- and inactive (−)-[^{11}C]DTBZ enantiomers (Koeppe *et al*, 1999). The PET studies using the inactive enantiomer also showed uniform cerebral distribution of free plus nonspecific uptake of (+)-[^{11}C]DTBZ (Koeppe *et al*, 1999).

In addition to VMAT2 binding of DTBZ, we estimated the blood-to-brain transport of DTBZ (K_1) in each imaged voxel from the initial 4-min scan frame ($C_{PET(0-4)}$) and the arterial plasma time course using the following equation:

$$C_{PET(0-4)} = \int_0^4 K_1 C_P(t) \otimes e^{-(K_1/DV_{tot})t} \quad (4)$$

where $\otimes$ represents the mathematical operation of convolution. No correction for tracer arrival time disparity between radial and carotid arteries was made. Procedurally, after calculation of the voxelwise total distribution volume (DV_{tot}), the blood to brain transport rate constant (K_1) was estimated voxel by voxel using an 'autoradiographic' approach proposed originally for estimation of blood flow (Herscovitch *et al*, 1983).

Striatal Volume-of-Interest Type-2 Vesicular Monoamine Transporter Binding Analyses

Peak BP activity was determined in striatal volumes of interest (VOI) representing the head of the CD, the anterior putamen (AP), and the posterior putamen (PP) using rectangular sampling regions measuring 4 (antero-posterior) × 2 (medio-lateral) × 1 (dorso-ventral) voxels (1 voxel = 2.25 mm^3). Data were extracted from images after linear transformation to Talairach space. Operationally, the transaxial image level best showing the head of the CD and the putamen was identified on the basis of the K_1 parametric images (approximately 0 to 5 mm above the AC–PC plane according to the atlas of Talairach and Tournoux, 1988). At this level, a 4-voxel-deep (antero-posterior) mediolateral sampling profile was centered over the head of the CD in the corresponding parametric DV_{tot} image. The 2-pixel-wide mediolateral maximum of the profile was then extracted from each hemisphere. Subsequently, the antero-posterior sampling profile was moved 4 voxels posteriorly to estimate DV_{tot} in AP, and then moved posteriorly again by 4 voxels to measure PP DV_{tot}. The DV_{tot} of the occipital cortex reference region was determined in a manually configured VOI applied at a transaxial level guided again by the K_1 parametric map.

For each striatal subregion, BP was calculated as described above (see equation (3)). The left and right sides were analyzed separately, then averaged within each subject to provide a BP for each subregion in each subject. Total putamen BP was computed by averaging AP and PP

values. To compute total striatal DTBZ BP, all three striatal subregions were averaged.

Anatomic Standardization and Voxel-Wise Analyses of Dihydrotetrabenazine K_1 and Tissue-to-Plasma Tracer Distribution Volume

Parametric K_1 and *DV* images were further anatomically standardized by nonlinear deformation ('warping') to the stereotaxic coordinate system of Talairach and Tournoux (1988) on the basis of the K_1 images, as described previously (Minoshima *et al*, 1994; Frey *et al*, 1996*b*). Volume of interest data were extracted from the standardized parametric K_1 images, using a predefined set of brain regions determined from the Talairach and Tourneaux atlas. Predefined volumes included all Brodmann areas and the major subcortical regions for both left and right hemispheres. In addition to these VOI analyses, we performed voxel-by-voxel analyses on the K_1 and DV ratio (*DVR*) images ($DVR = DV_{tot}/DV_{ns} = 1 + BP$).

Statistics

Age-related changes in normal subjects K_1 and *BP* were examined by linear and exponential regression analyses of parametric values with SYSTAT (Systat Software, Richmond, CA, USA), and the significance of intercept and slope parameter estimates were assessed by analysis of variance (ANOVA).

Regressions of K_1 and *BP* versus age were each performed in the normal subjects to assess regionally specific effects of aging. Striatal ROI DTBZ BP was assessed in PD subjects, employing age covariation as determined from the normal subjects. All comparisons of PD with normal subjects employed a subset of the normals with age similar to the PD subjects ($n = 51$; mean age 58 years; range 45 to 79 years; see Figure 1). Voxelwise analyses were performed on K_1 and *DVR* maps, unadjusted for effects of age. Significance of differences was assessed with unpaired, unequal variance, Student's *t*-tests.

Correlations between DTBZ BP and clinical status of PD subjects were investigated employing the Pearson correlation model with *post-hoc* significance assessed with the Bartlett χ^2 test as implemented in SYSTAT. Comparison of side-to-side clinical and striatal DTBZ binding asymmetries was assessed with relative asymmetry measures of $UPDRS_{III}$ and striatal ROI bindings. Asymmetry scores of $UPDRS_{III}$ questions with right and left components (items #20 to 26) were calculated by subtracting the left summed scores from right summed scores and normalizing by dividing with the aggregate sum of the left and right scores of these questions (final range of values = −1.0 to 1.0). A similar transformation was used for assessing DTBZ binding asymmetry. Left total striatal DTBZ binding deficit (difference between subject- and age-adjusted predicted normal total striatal DTBZ binding) was subtracted from the right total striatal DTBZ binding deficit and divided by the summed right and left striatal deficits (range of final values = −1.0 to 1.0).

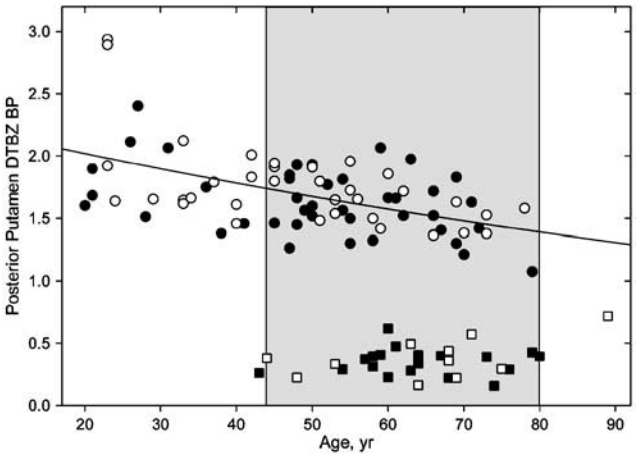

Figure 1 Posterior putamen DTBZ BP versus age in normal (filled circles = men; open circles = women) and PD subjects (filled squares = men, open squares = women). The line is the regression of PP DTBZ BP versus age in normal subjects using a declining exponential model (see Table 2). The shaded region indicates the subset of normal subjects used for group comparisons with PD. Within the normal group, there is a significant age-related decline in DTBZ BP. There is complete separation of normal and PD subject groups. There are no significant gender differences in normal or PD subjects.

Results

Blood–Brain Dihydrotetrabenazine Transport in Normal Aging and Parkinson Disease

Regression analyses of (+)-[^{11}C]DTBZ K_1 in normal subjects revealed an age-related global decline in ligand transport, averaging a 4.4% ± 1.4% loss per decade of life, consistent with the effect of the known normal age-related decline in cerebral blood flow (Leenders *et al*, 1990*a*). After removal of this global effect, no region changed by more than 2% per decade. Quantitative DTBZ K_1 estimates were not significantly different between PD and age-comparable normal subject groups either globally or in any of the atlas-based VOIs, though PD subjects averaged approximately 4% lower in cortical and 1% lower in subcortical structures than normal subjects. Voxel-by-voxel comparison of K_1 between PD and controls revealed significant reduction in parietal cortical K_1. Parametric K_1 images were also analyzed after normalization to each subject's global mean. Global mean K_1 was defined as the average of those voxels falling within 80% of the brain peak value. Statistical significance of the parietal cortex reduction in PD was enhanced in this analysis owing to reduced intersubject variance after removal of individual subject global K_1 effects. Volume of interest analysis of globally normalized K_1 values revealed significant, approximately 3% decreases in three regions (all in the parietal cortex); Brodmann areas 7, 39 and 40, with *P*-values less than 0.001, 0.004, and 0.001, respectively. No other VOI or voxels revealed significant differences in PD.

Type-2 Vesicular Monoamine Transporter Binding Sites in Normal Aging

Regression analyses of striatal (+)-[^{11}C]DTBZ VOI BP in normal subjects revealed age-related decline in VMAT2 binding sites in all striatal subregions (Figure 1, Table 2). Both linear and exponential models gave indistinguishable fits, revealing approximately 0.5% decline per year in DTBZ binding. Rates of decline were equivalent in all striatal subregions (Table 2). There was no effect of gender on DTBZ binding in any striatal subregion ($P > 0.09$).

Striatal Dihydrotetrabenazine Reductions in Parkinson Disease

There was no significant difference in occipital cortex DTBZ *DV* between PD and normal subjects. In PD subjects, the occipital cortex *DV* averaged 4.47 ± 0.92, while the *DV* of the PD-age-comparable normal subgroup was 4.84 ± 0.88 ($P = 0.08$ versus PD). It should be noted that the effect of the small reduction in the PD occipital cortex *DV* would be to relatively increase BP estimates (see equations (2) and (3)), thus potentially reducing, not enhancing, apparent deficits in PD striatal VMAT2 binding.

(+)-[^{11}C]Dihydrotetrabenazine BP was reduced significantly in all striatal VOI subregions of PD subjects (Table 3, Figure 1). There was complete separation between PD and normal subjects in (+)-[^{11}C]DTBZ BP in AP, PP, putamen, and in total striatum measures. In CD, there was one mildly affected (HY 1.0) PD subject whose BP values overlapped those of the normal subjects.

Voxel-by-voxel analysis of DTBZ DVR confirmed significant declines in binding throughout the PD striatum (Figure 2A), and additionally within the midbrain (Figure 2B). In the ventral midbrain, corresponding to the stereotaxic location of substantia nigra pars compacta (mediolateral: ± 6.5 mm; rostrocaudal: -18 mm; dorsoventral: -8 mm, in the reference space of Talairach and Tournoux, 1988), there were reductions approximating 50% of normal DTBZ binding, greatest on the brain side contralateral to the clinically most affected limbs. Ventral midbrain DTBZ binding correlates with ipsilateral CD significantly (most affected side, $r = 0.412$; $P < 0.05$, less affected side, $r = 0.524$; $P < 0.005$). There were no significant correlations with putaminal binding, probably due to floor effect in putaminal DVRs. In the dorsal midbrain, corresponding probably to the serotonergic raphe nuclei, there was no significant difference in DTBZ binding.

Intrastriatal Dihydrotetrabenazine Deficit Patterns in Parkinson Disease

In normal subjects, there was no significant striatal DTBZ BP difference between cerebral hemispheres.

Table 2 Effect of normal aging on striatal VOI DTBZ binding

Striatal region	*Intercept*	*Exponent*	F	P	*% loss/year*
CD	1.89 ± 0.17	0.0054 ± 0.0011	25.14	0.000004	0.54
AP	2.21 ± 0.15	0.0048 ± 0.0010	20.84	0.000020	0.48
PP	2.23 ± 0.16	0.0059 ± 0.0011	26.92	0.000002	0.59
Striatum	2.11 ± 0.15	0.0053 ± 0.0010	26.16	0.000002	0.53

Values represent constants from regression analyses based on an exponential model ($BP = Ae^{-Bt}$) using data from 75 normal subjects between the ages of 20 and 79 years. AP = anterior putamen; CD = caudate nucleus; PP = posterior putamen.

Table 3 Striatal VOI DTBZ binding deficits in parkinson disease

Striatal region	*Parkinson disease*	*Normal*	P	*Z-score*
Caudate nucleus, contralateral	0.610 ± 0.240	0.001 ± 0.169	1.35×10^{-16}	3.59
Caudate nucleus, ipsilateral	0.518 ± 0.244	-0.040 ± 0.183	5.44×10^{-15}	3.05
Anterior putamen, contralateral	1.140 ± 0.206	0.008 ± 0.198	2.45×10^{-34}	5.71
Anterior putamen, ipsilateral	1.029 ± 0.200	-0.051 ± 0.198	2.73×10^{-29}	5.45
Posterior putamen, contralateral	1.214 ± 0.173	0.007 ± 0.214	7.14×10^{-41}	5.64
Posterior putamen, ipsilateral	1.111 ± 0.192	-0.060 ± 0.211	7.11×10^{-37}	5.55
Putamen, contralateral	2.354 ± 0.357	0.016 ± 0.399	6.71×10^{-39}	5.86
Putamen, ipsilateral	2.140 ± 0.405	-0.111 ± 0.399	7.16×10^{-34}	5.65
Striatum, contralateral	0.989 ± 0.187	0.007 ± 0.176	3.15×10^{-32}	5.57
Striatum, ipsilateral	0.887 ± 0.202	-0.049 ± 0.186	3.80×10^{-29}	5.04

Values represent the means and s.d. of age-adjusted reductions in striatal DTBZ BP from Parkinson disease ($n = 31$) and normal subjects ($n = 51$) of comparable age ranges. The entire cohort of subjects was employed in the covariate adjustments, see Table 2. Deficits in the normal subjects should average 'zero' if the data from the broader age range are completely descriptive of the older normal subset. Indeed, the values are negligible in comparison to their variabilities and relative to the PD changes, confirming the validity of the covariation employed. Contralateral = striatum opposite the clinically most affected limbs. Ipsilateral = striatum ipsilateral to clinically most affected limbs. *Z*-score = [(PD mean−Normal mean)/Normal s.d.].

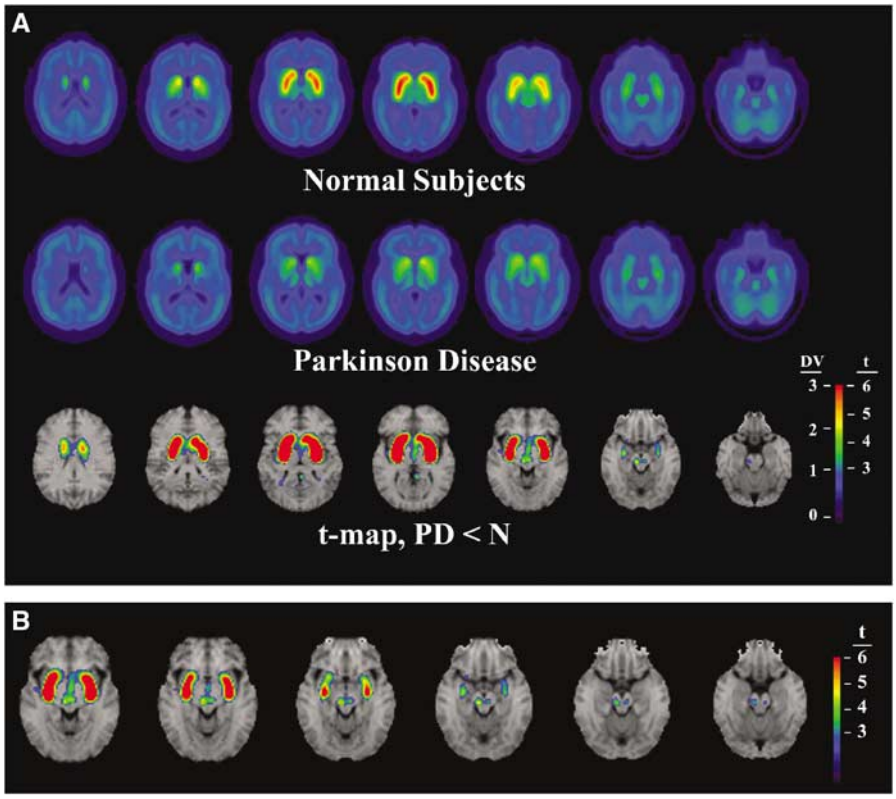

Figure 2 (**A**) Dihydrotetrabenazine binding in normal and PD subjects. Images depict group-average DTBZ DVR parametric maps in normal ($n = 51$, top row) and in PD subjects ($n = 31$, middle row). Individual images have been oriented before averaging so that the hemisphere contralateral to the most affected limbs (PD) or with the lowest striatal binding (normal subjects) is depicted on the image left. The pattern of significant reductions in PD is depicted superimposed on T1-weighted MRI for anatomic reference (bottom row). Images represent trans-axial levels from the vertex (left column) to the base (right column) of the brain at 10-mm intervals. The parametric images are presented in pseudocolor according to the scale at the bottom right (*DVR*: 0 to 3; *t*-statistic: 0 to 6). Striatal DTBZ binding is markedly decreased throughout the PD striatum, with the greatest change in the PP and least effect in the CD. The hemisphere contralateral to the clinically most affected body side has the greatest decrement in DTBZ binding. (**B**) Significant DTBZ DV reductions in the PD midbrain. Images show *t*-statistical maps superimposed on MRI for anatomical reference from upper (left image) to lower (right image) midbrain levels at contiguous 3.375-mm intervals. Differences correspond to the expected anatomic location of the substantia nigra, and are greatest contralateral (image left) to the most clinically affected body side.

Table 4 Intrastriatal VOI DTBZ BP patterns in parkinson disease

Striatal regional ratios	*Parkinson disease*	*Normal*	P	Z-*score*
CD C/I	0.90 ± 0.15	0.97 ± 0.05	1.05×10^{-02}	-1.39
AP C/I	0.85 ± 0.21	0.97 ± 0.04	4.65×10^{-03}	-2.56
PP C/I	0.80 ± 0.22	0.96 ± 0.06	5.36×10^{-04}	-2.81
Putamen C/I	0.83 ± 0.20	0.96 ± 0.04	8.44×10^{-04}	-3.41
Striatum C/I	0.86 ± 0.16	0.97 ± 0.02	6.99×10^{-04}	-4.77
Ipsilateral PP/CD	0.45 ± 0.15	1.14 ± 0.13	1.75×10^{-29}	-5.29
Contralateral PP/CD	0.51 ± 0.14	1.16 ± 0.11	6.52×10^{-28}	-5.94
Bilateral PP/CD	0.48 ± 0.13	1.15 ± 0.11	3.11×10^{-30}	-6.26

AP = anterior putamen; C/I = BP of the brain hemisphere contralateral to clinically most affected limbs divided by BP of the hemisphere ipsilateral to the most affected limbs; CD = caudate nucleus; contralateral = cerebral hemisphere contralateral to most affected limbs; ipsilateral = cerebral hemisphere ipsilateral to most affected limbs; PP = posterior putamen.

In contrast, PD subjects show significant asymmetries (Table 4, Figure 3). The ratios of subregional and total striatal DTBZ BP between the hemisphere contralateral to the clinically most affected limbs and the ipsilateral side were reduced significantly (Table 4). Analogous results were found in ratios of PP-to-CD DTBZ BP. These ratios were reduced significantly in PD subjects in contrast to normal

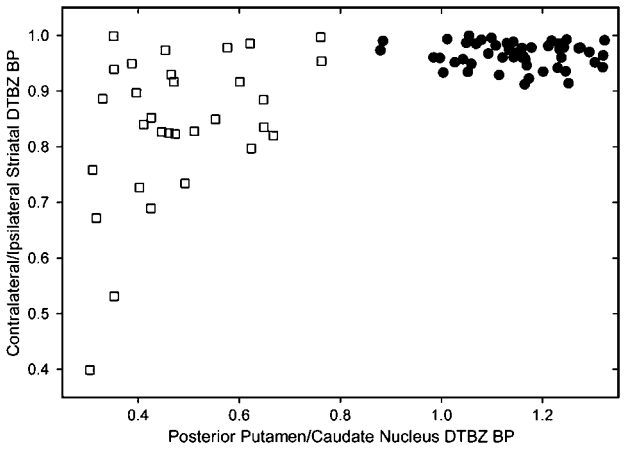

Figure 3 Intrastriatal DTBZ BP patterns in PD. Dihydrotetrabenazine BP ratios from striatal VOI are depicted for PD (squares) and normal (circles) subjects. Both the rostrocaudal and the side-to-side asymmetry patterns of BP differ significantly in PD. There is complete separation of PD subjects in the rostrocaudal pattern of BP loss.

subjects, where there was only a modest anterior-to-posterior increasing gradient (Table 4). Contralateral-to-ipsilateral and anterior-to-posterior (PP/CD) BP patterns differentiate PD and normal subject groups (Figure 3). The PP-to-CD ratio, in particular, exhibits complete separation of normal and PD subjects.

Clinical Correlates of Striatal Dihydrotetrabenazine in Parkinson Disease

In PD subjects, there were significant correlations between (+)-[^{11}C]DTBZ BP binding deficits and some clinical measures of disease status (Table 5, Figure 4). In CD, AP, PP and total striatum, (+)-[^{11}C]DTBZ BP deficits correlated significantly with disease duration. In CD, AP, and total striatum, DTBZ BP binding deficits correlated with SE ratings. There was no correlation in any striatal subregion or in the total striatum between DTBZ BP binding deficits and $UPDRS_{III}$ scores or HY stage.

Striata contralateral to the most clinically affected hemibody had the greatest decrements in DTBZ BP, and there was significant correlation between asymmetry indices of striatal DTBZ binding and $UPDRS_{III}$ scores ($r = 0.78$, $P < 0.0001$; Figure 5). In HY 1.0 and 1.5 subjects, PP DTBZ BP contralateral to the affected hemibody was decreased by 81%, while ipsilateral (clinically normal) PP DTBZ BP was diminished by 73% compared with normal subjects.

Discussion

The present study provides substantial evidence that (+)-[^{11}C]DTBZ-PET is suitable for quantification of the nigrostriatal projection, and, specifically, that it may constitute a biomarker of the projection in PD research. Dihydrotetrabenazine-PET depicts also the normal aging-related changes in striatal VMAT2 binding. In comparison with our prior studies employing racemic [^{11}C]DTBZ, we have observed the expected doubling of DVsp, an improvement in average striatal DV_{sp} to DV_{tot} ratio to $\sim$75% in normal subjects. This improved specificity permits better depiction of extrastriatal binding, as exemplified by our current findings in the midbrain.

Our current implementation of VMAT2 estimation with DTBZ employed continuous intravenous infusion and steady-state analysis. We have reported previously that a reference tissue ROI approach can be employed with DTBZ, and that the occipital cortex region is satisfactory for this purpose (Koeppe *et al*, 1999). The present results underscore the lack of significant effect of PD on the occipital cortex, obviating the need for blood sampling in future studies of PD.

Table 5 Clinical correlations of striatal VOI DTBZ binding deficits in parkinson disease

Striatal region	*Duration*	*Hoehn and Yahr*	*Schwab and England*	*$UPDRS_{III}$*
CD	0.542**	0.335	−0.403*	0.326
AP	0.514**	0.131	−0.373*	0.203
PP	0.377*	−0.123	−0.232	0.030
Striatum	0.529**	0.144	−0.376*	0.212

Pearson correlation coefficients of bilaterally averaged, age-adjusted DTBZ BP reductions and clinical measures in 31 PD patients. AP = anterior putamen; CD = caudate nucleus; PP = posterior putamen; striatum = average of CD, AP, and PP. *$P < 0.05$; **$P < 0.005$.

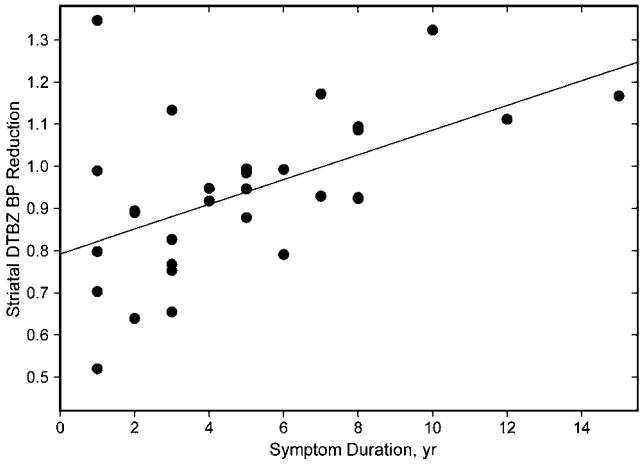

Figure 4 Disease duration versus age-adjusted total striatal DTBZ BP binding deficit in PD. The duration of clinical symptoms correlates significantly with the total striatal BP reduction averaged over both hemispheres (BP reduction = 0.7923 + 0.0294 × year; $r^2 = 0.2795$).

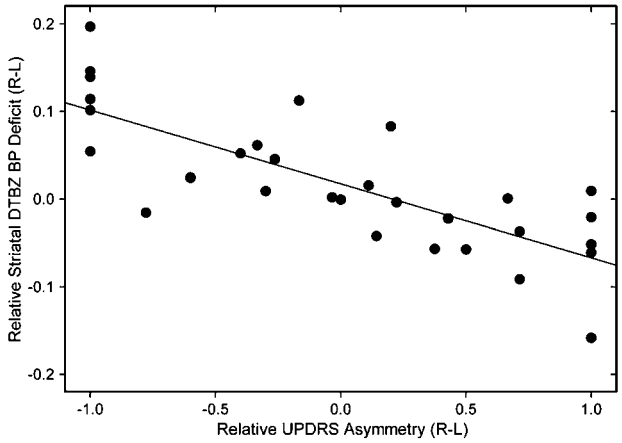

Figure 5 Relative clinical asymmetry ($UPDRS_{III}$) versus relative total striatal DTBZ BP deficit asymmetry in PD. The relative right–left hemisphere (BP deficit) and body motor impairment (UPDRS) values in each subject were expressed relative to the total (bilateral sum) deficits in each PD subject, yielding a relative estimate of side-to-side pathological asymmetry. There is significant correlation of DTBZ binding and clinical motor asymmetry in PD (DTBZ $BP = 0.0173 - 0.0842 \times UPDRS$; $r^2 = 0.6044$).

Normal Nigrostriatal Aging

The magnitude of decline associated with normal age in striatal VMAT2 binding sites in the present study is similar to results obtained with a variety of other methods, including postmortem assays of nigral neuron loss with normal aging, postmortem *in vitro* studies of nigrostriatal terminal integrity, and prior *in vivo* imaging studies (McGeer *et al*, 1977; Zelnik *et al*, 1986; Scherman *et al*, 1989; Fearnley and Lees, 1991; DeKeyser *et al*, 1990; Volkow *et al*, 1994; van Dyck *et al*, 1995). Conversely, a recent postmortem study of age-related changes in human striatal dopaminergic markers found no evidence of age-related decline in striatal VMAT2 expression (Haycock *et al*, 2003), but this study had a significantly smaller number of subjects over the age of 20 than ours, and postmortem measurements might be confounded by agonal and postmortem changes in VMAT2 levels, increasing variation and reducing the chance of finding an age-related change.

Basal Ganglia Type-2 Vesicular Monoamine Transporter Binding Changes in Parkinson Disease

We found no overlap of DTBZ BP ranges in AP, PP or total striatal DTBZ binding sites between PD and normal subjects. Specific PP (+)-[^{11}C]DTBZ binding was most reduced and CD binding least affected in PD. Nevertheless, there was near complete separation in CD DTBZ binding between PD and normal subjects, with only one minimally symptomatic PD subject (HY stage 1) overlapping the normal range. We did not use anatomic MRI for anatomic adjustment or atrophy correction. While there is age-related change in regional brain volumes that can be depicted by brain MRI, there are no significant differences in striatal volumes between control and medication-responsive PD subjects. We conclude that the losses in DBTZ binding in PD subjects reflect nigrostriatal damage rather than atrophy (Good *et al*, 2001; Schulz *et al*, 1999; Burton *et al*, 2004; Summerfield *et al*, 2005).

Parkinson disease alters also the subregional pattern of striatal DTBZ binding. Dihydrotetrabenazine BP is normally symmetric between hemispheres, while in PD there is significant asymmetry of binding, with reduction greatest in the striatum contralateral to the clinically most affected limbs. The normal rostrocaudal gradient of increasing DTBZ binding is also altered in PD, where a marked decline in the ratio of PP-to-CD DTBZ binding is observed. Our results are consistent with findings in postmortem VMAT2 binding assays, showing near-complete losses of specific VMAT2 binding in the PP in more advanced PD subjects (Scherman *et al*, 1989; Lehéricy *et al*, 1994) and more prominent nigrostriatal projection lesions in the PP of less severely affected PD subjects (Kish *et al*, 1988; Fearnley and Lees, 1991; Damier *et al*, 1999; German *et al*, 1989; Gibb *et al*, 1990).

Striatal DTBZ binding changes are correlated with ventral midbrain reductions in PD subject binding, corresponding to the coordinates of the substantia nigra and reduced greatest contralateral to the most clinically affected limbs. This result is noteworthy since normal BPs in the midbrain are approximately 0.3, indicating that only $\sim$25% of total DTBZ uptake in this region is due to specific binding. Parkinson disease subject dorsal midbrain, probably corresponding to the serotonergic raphe nuclei (Zubieta *et al*, 2000), was not different statistically from age-matched normals. Although postmortem studies show loss of serotonergic neurons in PD (Hornykiewicz and Kish, 1987; Chinaglia *et al*, 1993), our result suggests that serotonergic neuron degeneration might be a later feature of PD.

Our results are in good agreement with postmortem studies, suggesting 70 to 80% losses of PP dopamine (Kish *et al*, 1988; Bernheimer *et al*, 1973) and perhaps somewhat lesser losses of nigral neurons (Fearnley and Lees, 1991; Damier *et al*, 1999) when symptoms of PD are initially manifest. We were able to assess the DTBZ deficit accompanying the clinical 'threshold' of PD by examination of binding contralateral to the clinically unaffected side in HY 1 and 1.5 subjects. In these subjects, we found 73% loss of PP DTBZ binding in the 'unaffected' PP. The DTBZ binding 'threshold' for development of clinical parkinsonism is therefore between this value and that of the 'affected' side (81% loss) in these most mildly affected subjects.

K_1/Regional Cerebral Blood Flow Changes

In contrast to DTBZ-binding data, there were no differences between PD subjects and age-comparable normals in striatal K_1 values. Voxel-by-voxel and VOI analysis, however, showed significant decreases in PD parietal cortex. Since DTBZ K_1 largely reflects regional cerebral blood flow, it may constitute an indirect measure of regional brain 'functional' and energy metabolic activity (Koeppe *et al*, 2005). Prior FDG-PET studies of regional cerebral metabolism in PD show hypometabolism in the cerebral cortex (Peppard *et al*, 1992; Eberling *et al*, 1994; Piert *et al*, 1996; Vander Borght *et al*, 1997; Bohnen *et al*, 1999). Prior studies have, however, usually shown more widespread reductions involving the occipital and posterior cingulate cortices in addition to the parietal association area (Peppard *et al*, 1992; Eberling *et al*, 1994; Piert *et al*, 1996; Vander Borght *et al*, 1997; Bohnen *et al*, 1999). We did find evidence of widespread reductions in regional cortical K_1, but these differences did not attain significance with the relatively stringent statistical thresholds we employed (data not shown). Our data are consistent also with the results of Eidelberg *et al* (1990, 1994) and Fukuda *et al* (2001), who have described a 'network pattern' of regional metabolic covariations in PD using a variation of principal component analysis. In this analysis, parietal association cortex is identified as an area of relative metabolic reduction covarying with increases in the striatum and pallidum and with decreases in the thalamus and prefrontal and occipital cortices.

Dihydrotetrabenazine-Positron Emission Tomography Versus Other Nigrostriatal Dopamine Terminal Markers

Estimates of DA nerve terminal loss in PD are dependent partly on the marker selected (Wilson *et al*, 1996*b*). Estimates of AADC activity with [^{18}F]FDOPA suggest more modest nigrostriatal losses than do our VMAT2 results. [^{18}F]6-fluorodopa uptake (K_i) values in mild PD often exceed 50% of normal putaminal values with significant overlap of values in normal subjects and PD patients (Sawle *et al*, 1994; Morrish *et al*, 1996*b*). Considerable experimental evidence suggests that AADC activity is regulated by extracellular dopamine levels via activation of dopamine D2 receptors (Hadjiconstantinou *et al*, 1993; Young *et al*, 1993; Cumming *et al*, 1995; Tedroff *et al*, 1999). Relative preservation of FDOPA K_i in PD striatum may result from upregulation of AADC activity in response to the loss of dopaminergic terminals (Kish *et al*, 1995; Wilson and Kish, 1996*a*; Tedroff *et al*, 1999; Lee *et al*, 2000). Although striatal AADC activity as measured by FDOPA K_i has good correlation with clinical measures of disease severity and with postmortem nigral neuron counts, it might be relatively insensitive to earlier changes in PD (Ishikawa *et al*, 1996) and be affected by dopaminergic drug treatment, reducing its usefulness as an objective measure of nigrostriatal terminal density.

Use of DAT ligands may have analogous pitfalls. In common with numerous other cell surface proteins, DAT molecules cycle between the cell surface membrane and endosomal compartments. Within endosomal compartments, DAT molecules may have reduced affinity for cocaine analogue tracers, leading to an apparent reduction in the number of binding sites (Zhu *et al*, 1997; Doolen and Zahniser, 2001). Dopamine receptor activation may regulate the distribution of DAT molecules between the cell membrane and endosomes (Batchelor and Schenk, 1998). Lee *et al* (2000) presented data that DAT binding sites are downregulated in PD striatum and Guttman *et al* (2001) presented data that dopaminomimetic agents downregulate striatal DAT binding in early PD subjects.

The potential regulation of FDOPA uptake and DAT binding by loss of striatal dopamine terminals and dopaminergic drugs requires cautious interpretation of FDOPA and DAT imaging data from neuroprotection trials. In the imaging substudy of the CALM-PD study comparing initial pramipexole with initial levodopa therapy, subjects receiving initial pramipexole therapy were reported to have relative preservation of striatal DAT binding when subjects were compared at 22, 34, and 46 months after randomization. Clinical measures of disease status, however, were identical at 46 months (Parkinson Study Group, 2002). The effect of pramipexole on DAT binding, moreover, appeared in the initial randomization to 22-month interval, and there was no evidence of a sustained neuroprotective effect, consistent with a pharmacologic effect on DAT expression after initiation of treatment (Albin *et al*, 2002; Albin and Frey, 2003; Ahlskog, 2003). Guttman *et al* (2001) suggested that levodopa had a greater effect on downregulating DAT binding than dopamine agonists, which would be consistent with the CALM-PD imaging results. Analogous results were obtained in the ELLDOPA study of possible levodopa toxicity. In ELLDOPA, a placebo-treated group was compared with two schedules of levodopa treatment for 40 weeks and a subset of subjects underwent single photon emission computed tomography (SPECT) imaging with the DAT ligand β-CIT at entry and conclusion of the trial (Parkinson Study Group, 2004). The greatest decrement in DAT binding was found in the highest levodopa treatment group, though this group had the best clinical ratings of disease severity, even when evaluated after a 2-week treatment washout. The discrepancy between imaging and clinical results is a possible reflection of levodopa treatment regulation of DAT binding and/or the long-duration clinical effects of levodopa treatment (Hauser *et al*, 2000). In a third recent neuroprotection study, REAL-PET, FDOPA imaging was used to assess the

differences in disease status between initial ropinirole- and initial levodopa-treated subjects (Whone *et al*, 2003). As with the CALM-PD substudy, the initial dopamine agonist group had a significantly smaller decrement in FDOPA uptake than the initial levodopa treatment group. Comparison with clinical measures was not possible; subjects were not evaluated in the 'off' state at the conclusion of the trial. Unified Parkinson Disease Rating Scale ratings during the study, however, favored the initial levodopa-treated group, suggesting greater intensity of treatment in the initial levodopa-treated group. It is possible that the measured differences in AADC activity between the two arms of REAL-PET reflect a pharmacologic difference due to differential AADC regulation by differing treatment intensity rather than a difference in rate of nigrostriatal terminal degeneration.

The majority of available evidence indicates that striatal VMAT2 binding sites do not undergo up- or downregulation under conditions that alter the synthesis or turnover of dopamine in experimental animals (Naudon *et al*, 1994; Vander Borght *et al*, 1995*b*; Kilbourn *et al*, 1996; Wilson *et al*, 1996*b*; Zucker *et al*, 2001; Kemmerer *et al*, 2003). This is true in the normal striatum, the partially dopamine denervated striatum, and also in the massively dopamine denervated striatum. Similar results have been obtained in serotonergic pathways with manipulations of serotonergic neurotransmission (Vilpoux *et al*, 2000). Type-2 vesicular monoamine transporter transporter activity and its subcellular distribution within nerve terminals might, however, be regulated actively by monoaminergic neurotransmitter actions (Holtje *et al*, 2003; Fleckstein and Hanson, 2003; Truong *et al*, 2003; Ugarte *et al*, 2003). The changing distribution of VMAT2 among different compartments of striatal nerve terminals, however, does not alter total striatal VMAT2 binding as measured with radiolabeled tetrabenazine analogues (reviewed in Fleckstein and Hanson, 2003; Hogan *et al*, 2000). These preclinical studies suggest that DTBZ-PET provides an anatomic marker of nigrostriatal terminal density that is not readily influenced by alterations in dopaminergic neurotransmission. Human imaging experiments examining directly the possible regulation of DBTZ binding by dopaminergic agents remain to be performed. De La Fuente-Fernandez *et al* (2003) presented DTBZ-PET data indicating increased binding in the striata of individuals with dopa-responsive dystonia, which could indicate dopaminergic regulation of VMAT2 expression. An alternative explanation is that dopamine absence within synaptic vesicles exposes more tetrabenazine analogue binding sites due to lack of competition for the common binding site (De La Fuente-Fernandez *et al*, 2003). If lack of direct regulation by dopaminomimetic treatments is shown in PD, an additional practical advantage of *in vivo* VMAT2 assays is that measures can be performed without discontinuation of symptomatic dopaminergic therapy, as indicated by recent preclinical studies (Kilbourn *et al*, 1996).

Relationship of Nigrostriatal Imaging to Clinical Measures

Striatal FDOPA uptake is correlated with clinical measures of disease severity, particularly bradykinesia (Eidelberg *et al*, 1990; Antonini *et al*, 1995; Morrish *et al*, 1996*a*; Vingerhoets *et al*, 1997), and DAT losses as assessed by [^{123}I]β-CIT are correlated with the stage and severity of PD (Seibyl *et al*, 1995; Pirker, 2003). We also find correlations between striatal DTBZ binding and clinical measures of PD severity and asymmetry. We find that the duration of symptoms and SE ratings correlated with total striatal and subregional DTBZ binding. The highest correlations were with the DTBZ BP deficits in the CD and AP. The lack of correlations between clinical ratings and VMAT2 binding in the PP probably reflects a 'floor' effect because of the marked losses of PP DA innervation before the time of clinically manifest PD (Antonini *et al*, 1995; Seibyl *et al*, 1995; Vingerhoets *et al*, 1997). Our subject selection and limitations of clinical measures may contribute also to the absence of some correlations, notably the HY and $UPDRS_{III}$ ratings. In studies reporting significant correlations between FDOPA uptake or DAT binding and clinical measures such as the HY scale and $UPDRS_{III}$, a wider range of subjects (HY 1 to 5) was studied (reviewed in Pirker, 2003). Our study of only HY 1 to 3 subjects limits the range available for correlation. If prior studies had been restricted to HY 1 to 3 subjects, it is possible that no significant correlations between tracer binding measures and clinical scales would have been observed. The [^{123}I]β-CIT study of Pirker (2003), for example, would probably not show a correlation between UPDRS scores and binding measures if HY stage 4 and 5 subjects were eliminated. In addition, the HY scale is a relatively crude disease index and distinction between HY 2 and HY 3 might be subtle. The most widely used quantitative clinical measure in PD is the UPDRS scale, and particularly the $UPDRS_{III}$ subscale. This measure possesses considerable intrinsic variation and is altered by symptomatic treatment effects, even when used in the practically defined 'off' state (Hauser *et al*, 2000; Holloway and Dick, 2002). In particular, the variable long duration effect of levodopa and use of relatively long half-life dopamine agonists can confound interpretation of the 'off' $UPDRS_{III}$.

Clinical measures, such as time until need for levodopa treatment or change in UPDRS ratings, have been the primary tools for evaluating potential neuroprotective interventions (Holloway and Dick, 2002). Drawbacks of these measures include considerable variability, the confounding effects of dopaminomimetic treatments, and potential symptomatic effects of putatively neuroprotective treat-

ments themselves. In addition, the relationship between clinical manifestations and underlying pathology is complex. Clinically manifest parkinsonism, for example, appears only when approximately 75% of PP nigrostriatal terminals are lost. Clinical measures reflect admixtures of the degree of underlying pathology, treatment effects, and the activity of poorly understood compensatory processes. In their cogent critique, Holloway and Dick (2002) point out that conventional clinical measures such as the UPDRS or time to some change in clinical status (e.g. need for dopaminomimetic treatment or emergence of motor fluctuations) are themselves putative surrogate biomarkers of disease progression rather than validated clinical endpoints.

A biomarker that reflects objectively the progression of pathology in PD would be an invaluable aid for evaluating potential neuroprotective interventions. Brooks *et al* (2003) presented explicit criteria for a suitable biomarker of disease progression. Molecular imaging methods, such as FDOPA-PET imaging, DAT-PET or -SPECT imaging, and VMAT2-PET imaging, satisfy almost all the criteria for a suitable biomarker. However, an important exception is the likely regulation of AADC activity and DAT distribution by partial striatal dopaminergic denervation and by dopaminomimetic agents, which potentially confound interpretation of FDOPA and β-CIT imaging studies. Preclinical studies of VMAT2 expression suggest that it is not subject to these regulatory limitations, and that (+)-[^{11}C]DTBZ-PET is a suitable candidate for the objective quantification of nigrostriatal integrity in PD. The present studies confirm and extend observations that VMAT2-PET imaging depicts the severity and distribution of nigrostriatal lesions in PD, in keeping with clinical and behavioral measures. Final evaluation of the suitability of (+)-[^{11}C]DTBZ-PET as a PD biomarker will require direct assessment of the effects of dopaminomimetic agents in previously unmedicated PD subjects.

Acknowledgements

The authors thank The University of Michigan PET technologists for their skillful performance in data acquisition and the cyclotron operators and radiochemists for their reliable production of (+)-DTBZ.

References

Ahlskog JE (2003) Slowing Parkinson's disease progression: recent dopamine agonist trials. *Neurology* 60: 381–389

Albin RL, Frey KA (2003) Initial agonist treatment of Parkinson disease: a critique. *Neurology* 60:390–4

Albin RL, Koeppe RA, Chervin RD, Consens FB, Wernette K, Frey KA *et al* (2000) Decreased striatal dopaminergic innervation in REM sleep behavior disorder. *Neurology* 55:1410–2

Albin RL, Nichols TE, Frey KA (2002) Brain imaging to assess the effects of dopamine agonists on progression of Parkinson's disease (letter to the editor). *JAMA* 288:311–2

Antonini A, Vontobel P, Psylla M, Günther I, Maguire RP, Missimer J *et al* (1995) Complementary positron emission tomographic studies of the striatal dopaminergic system in Parkinson's disease. *Arch Neurol* 52:1183–90

Batchelor M, Schenk JO (1998) Protein kinase A activity may kinetically upregulate the striatal transporter for dopamine. *J Neurosci* 18:10304–9

Bernheimer H, Birkmayer W, Hornykiewicz O *et al* (1973) Brain dopamine and the syndromes of Parkinson and Huntington. Clinical, morphological and neurochemical correlations. *J Neurol Sci* 20:415–55

Bohnen NI, Minoshima S, Giordani B, Frey KA, Kuhl DE (1999) Motor correlates of occipital glucose hypometabolism in Parkinson's disease without dementia. *Neurology* 53:541–8

Brooks DJ, Frey KA, Marek KL *et al* (2003) Assessment of neuroimaging techniques as biomarkers of the progression of Parkinson's disease. *Exp Neurol* 184:S68–79

Burton EJ, McKeith IG, Burn DJ, Williams ED, O'Brien JT (2004) Cerebral atrophy in Parkinson's disease with and without dementia: a comparison with Alzheimer's disease, dementia with Lewy bodies and controls. *Brain* 127:791–800

Chinaglia G, Alvarez FJ, Probst A, Palacios JM (1992) Mesostriatal and mesolimbic dopamine uptake binding sites are reduced in Parkinson's disease and progressive supranuclear palsy: a quantitative autoradiographic study using [^{3}H]mazindol. *Neuroscience* 49:317–27

Chinaglia G, Landwehrmeyer B, Probst A, Palacios JM (1993) Serotoninergic terminal transporters are differentially affected in Parkinson's disease and progressive supranuclear palsy: an autoradiographic study with [^{3}H]citalopram. *Neurosci* 54:691–9

Cumming P, Kuwabara H, Ase A, Gjedde A (1995) Regulation of DOPA decarboxylase activity in brain of living rat. *J Neurochem* 65:1381–90

Damier P, Hirsch EC, Agid Y, Graybiel AM (1999) The substantia nigra of the human brain. II. Patterns of loss of dopamine-containing neurons in Parkinson's disease. *Brain* 122:1437–48

Daniels GM, Amara SG (1999) Regulated trafficking of the human dopamine transporter. Clathrin-mediated internalization and lysosomal degradation in response to phorbol esters. *J Biol Chem* 274:35794–801

De La Fuente-Fernandez R, Furtado S, Guttman M, Furukawa Y, Lee CS, Calne DB *et al* (2003) VMAT2 binding is elevated in dopa-responsive dystonia: visualizing empty vesicles by PET. *Synapse* 49: 20–28

DeKeyser J, Ebinger G, Vauquelin G (1990) Age-related changes in the human nigrostriatal system. *Ann Neurol* 27:157–61

Doolen S, Zahniser NR (2001) Protein tyrosine kinase inhibitors alter human dopamine transporter activity in *Xenopus* oocytes. *J Pharmacol Exp Thera* 296:931–8

Eberling JL, Richardson BC, Reed BR, Wolfe N, Jagust WJ (1994) Cortical glucose metabolism in Parkinson's disease without dementia. *Neurobiol Aging* 15: 329–335

Eidelberg D, Moeller JR, Dhawan V *et al* (1994) The metabolic topography of parkinsonism. *J Cereb Blood Flow Metab* 14:783–801

Eidelberg D, Moeller JR, Dhawan V, Sidtis JJ, Ginos JZ, Strother SC *et al* (1990) The metabolic anatomy of Parkinson's disease: complementary [^{18}F]fluorodeoxyglucose and [^{18}F]fluorodopa positron emission tomographic studies. *Mov Disord* 5:203–13

Erickson JD, Eiden LE (1993) Functional identification and molecular cloning of a human brain vescile monoamine transporter. *J Neurochem* 61:2314–7

Fahn S, Elton R, Members of the UPDRS Development Committee (1987) Unified Parkinson's disease rating scale. In: *Recent developments in parkinson's disease* (Fahn S, Marsden CD, Calne DB, Goldstein M, eds), Florham Park, NJ: Macmillan Healthcare Information, 153–64

Fearnley JM, Lees AJ (1991) Ageing and Parkinson's disease: substantia nigra regional selectivity. *Brain* 114:2283–301

Fleckstein AE, Hanson GR (2003) Impact of psychostimulants on vesicular monoamine transporter function. *Eur J Pharmacol* 479:283–9

Frey KA, Koeppe RA, Mulholland GK *et al* (1992) *In vivo* muscarinic cholinergic receptor imaging in human brain with [^{11}C]scopolamine and positron emission tomography. *J Cereb Blood Flow Metab* 12:147–54

Frey KA, Koeppe RA, Kilbourn MR, Vander Borght TM, Albin RL, Gilman S *et al* (1996*a*) Presynaptic monoaminergic vesicles in Parkinson's disease and normal aging. *Ann Neurol* 40:873–84

Frey KA, Minoshima S, Koeppe RA, Kilbourn MR, Berger KL, Kuhl DE (1996*b*) Stereotaxic summation analysis of human cerebral benzodiazepine binding maps. *J Cereb Blood Flow Metab* 16:409–17

Frost JJ, Rosier AJ, Reich SG *et al* (1993) Positron emission tomographic imaging of the dopamine transporter with ^{11}C-WIN 35,428 reveals marked declines in mild Parkinson's disease. *Ann Neurol* 34:423–31

Fukuda M, Edwards C, Eidelberg D (2001) Functional brain networks in Parkinson's disease. *Parkinsonism Relat Disord* 8:91–4

Garnett ES, Firnau G, Nahmias C (1983) Dopamine visualized in the basal ganglia of living man. *Nature* 305:137–8

Gelb DJ, Oliver E, Gilman S (1999) Diagnostic criteria for Parkinson disease. *Arch Neurol* 56:33–9

German DC, Manaye K, Smith WK, Woodward DJ, Saper CB (1989) Midbrain dopaminergic cell loss in Parkinson's disease: computer visualization. *Ann Neurol* 26:507–14

Gibb WRG, Fearnley JM, Lees AJ (1990) The anatomy and pigmentation of the human substantia nigra in relation to selective neuronal vulnerability. *Adv Neurol* 53:31–4

Gilman S, Frey KA, Koeppe RA, Junck L, Little R, Vander Borght M *et al* (1996) Decreased striatal monoaminergic terminals in olivopontocerebellar atrophy and multiple system atrophy demonstrated with positron emission tomography. *Ann Neurol* 40:885–92

Good CD, Johnsrude IS, Ashburner J, Henson RNA, Friston KJ, Frackowiack RSJ (2001) A voxel-based morphometric study of ageing in 465 normal adult human brains. *NeuroImage* 14:21–36

Greengard P, Valtorta F, Czernik AJ, Benfenati F (1993) Synaptic vesicle phosphoproteins and regulation of synaptic function. *Science* 259:780–5

Guttman M, Stewart D, Hussey D, Wilson A, Houle S, Kish S (2001) Influence of L-dopa and pramipexole on striatal dopamine transporter in early PD. *Neurology* 56:1559–64

Hadjiconstantinou M, Wemlinger TA, Sylvia CP *et al* (1993) Aromatic amino acid decarboxylase activity of mouse striatum is modulated via dopamine receptors. *J Neurochem* 60:2175–80

Hauser RA, Koller WC, Hubble JP *et al* (2000) Time course of loss of clinical benefit following withdrawal of levodopa/carbidopa and bromocriptine in early Parkinson's disease. *Mov Disord* 15:484–9

Haycock JW, Becker L, Ang L, Furukawa Y, Hornykiewicz O, Kish SJ (2003) Marked disparity between age-related changes in dopamine and other presynaptic dopaminergic markers in human striatum. *J Neurochem* 87:574–85

Herscovitch P, Markham J, Raichle ME (1983) Brain blood flow measured with intravenous H_2O^{15}. I. Theory and error analysis. *J Nucl Med* 24:782–9

Hoehn M, Yahr MP (1967) Onset, progression, and mortality. *Neurology* 17:427–42

Hogan KA, Staal RGW, Sonsalla PK (2000) Analysis of VAMT2 binding after methamphetamine or MPTP treatment: disparity between homogenates and vesicle preparations. *J Neurochem* 74:2217–20

Holloway RG, Dick AW (2002) Clinical trial endpoints: on the road to nowhere? *Neurology* 58:679–86

Holtje M, Winter S, Walther D *et al* (2003) The vesicular monoamine content regulates VMAT2 activity through $G\alpha_q$ in mouse platelets: evidence for autoregulation of vesicular transmitter uptake. *J Biol Chem* 278:15850–8

Hornykiewicz O, Kish SJ (1987) Biochemical pathophysiology of Parkinson's disease. *Adv Neurol* 45:19–34

Ishikawa T, Dhawan V, Chaly T, Margouleff C, Robeson W, Dahl RJ *et al* (1996) Clinical significance of striatal DOPA decarboxylase activity in Parkinson's disease. *J Nucl Med* 37:216–22

Jewett DM, Kilbourn MR, Lee LC (1997) A simple synthesis of [^{11}C]dihydrotetrabenazine (DTBZ). *Nucl Med Biol* 24:197–9

Kaufman MJ, Madras BK (1991) Severe depletion of cocaine recognition sites associated with the dopamine transporter in Parkinson's-diseased striatum. *Synapse* 9:43–9

Kemmerer ES, Desmond TJ, Albin RL, Kilbourn MR, Frey KA (2003) Treatment effects on nigrostriatal projection integrity in partial 6-OHDA lesions: comparison of L-DOPA and pramipexole. *Exp Neurol* 183:81–6

Kilbourn M, Lee L, Vander Borght T, Jewett D, Frey K (1995) Binding of α-dihydrotetrabenazine to the vesicular monoamine transporter is stereospecific. *Eur J Pharmacol* 278:249–52

Kilbourn MR, Frey KA, Vander Borght T, Sherman PS (1996) Effects of dopaminergic drug treatments on *in vivo* radioligand binding to brain monoamine transporters. *Nucl Med Biol* 23:467–71

Kilbourn MR (1997) *In vivo* radiotracers for vesicular neurotransmitter transporters. *Nucl Med Biol* 24:615–9

Kish SJ, Shannak K, Hornykiewicz O (1988) Uneven pattern of dopamine loss in the striatum of patients with idiopathic Parkinson's disease. *N Engl J Med* 318:876–80

Kish SJ, Zhong XH, Hornykiewicz O, Haycock JW (1995) Striatal 3,4-dihydroxyphenylalanine decarboxylase in aging: disparity between postmortem and positron emission tomographic studies? *Ann Neurol* 38:260–4

Koeppe RA, Frey KA, Kuhl DE, Kilbourn MR (1999) Assessment of extrastriatal vesicular monoamine trans-

porter binding site density using stereoisomers of [11C]dihydrotetrabenazine. *J Cereb Blood Flow Metab* 19:1376–84

Koeppe RA, Frey KA, Kume A, Albin R, Kilbourn MR, Kuhl DE (1997) Equilibrium versus compartmental analysis for assessment of the vesicular monoamine transporter using (+)-[11C]dihydrotetrabenazine (DTBZ) and positron emission tomography. *J Cereb Blood Flow Metab* 17:919–31

Koeppe RA, Gilman S, Joshi A, Liu S, Little R, Junck L *et al* (2005) [11C]DTBZ and [18F]FDG PET measures in differentiating dementias. *J Nucl Med* 46:936–44

Lammertsma AA, Bench CJ, Hume SP, Osman S, Gunn K, Brooks DJ *et al* (1996) Comparison of methods for analysis of clinical [11C]raclopride studies. *J Cereb Blood Flow Metab* 16:42–52

Lee CS, Samii A, Sossi A, Ruth TJ, Schulzer M, Holden JE *et al* (2000) *In vivo* positron emission tomographic evidence for compensatory changes in presynaptic dopaminergic nerve terminals in Parkinson's disease. *Ann Neurol* 47:493–503

Leenders KL, Perani D, Lammertsma AA *et al* (1990*a*) Cerebral blood flow, blood volume and oxygen utilization. Normal values and effect of aging. *Brain* 113:27–47

Leenders KL, Salmon EP, Tyrrell P *et al* (1990*b*) The nigrostriatal dopaminergic system assessed *in vivo* by positron emission tomography in healthy volunteer subjects and patients with Parkinson's disease. *Arch Neurol* 47:1290–8

Lehéricy S, Brandel J-P, Hirsch EC *et al* (1994) Monoamine vesicular uptake sites in patients with Parkinson's disease and Alzheimer's disease, as measured by tritiated dehydrotetrabenazine autoradiography. *Brain Res* 659:1–9

McGeer PL, McGeer EG, Suzuki JS (1977) Aging and extrapyramidal function. *Arch Neurol* 34:33–5

Meiergerd SM, Hooks SM, Schenk JO (1994) The striatal transporter for dopamine in the rat may be kinetically up-regulated following 3 weeks of withdrawal form cocaine self administration. *J Neurochem* 63:1277–81

Melikian HE, Buckley KM (1999) Membrane trafficking regulates the activity of the human dopamine transporter. *J Neurosci* 19:7699–710

Minoshima S, Koeppe RA, Fessler JA, Mintun MA, Berger KL, Taylor SF *et al* (1993*b*) Integrated and automated data analysis method for neuronal activation studies using 0^{15} water PET. In: *Quantification of brain function totracer kinetics and image analysis in brain PET* (Uemura K, Lassen NA, Jones T, Kanno I, eds), International Congress Series 1030, Tokyo: Excerpta Medica, 409–18

Minoshima S, Koeppe RA, Frey KA, Kuhl DE (1994) Anatomic standardization: linear scaling and nonlinear warping of functional brain images. *J Nucl Med* 35:1528–37

Minoshima S, Koeppe RA, Mintun MA, Berger KL, Taylor SF, Frey KA *et al* (1993*a*) Automated detection of the intercommissural line for stereotactic localization of functional brain images. *J Nucl Med* 34:322–9

Mintun MA, Raichle ME, Kilbourn MR, Wooten GF, Welch MJ (1984) A quantitative model for the *in vivo* assessment of drug binding sites with positron emission tomography. *Ann Neurol* 15:217–27

Morrish PK, Sawle GV, Brooks DJ (1996*a*) An [18F]dopa-PET and clinical study of the rate of progression in Parkinson's disease. *Brain* 119:585–91

Morrish PK, Sawle GV, Brooks DJ (1996*b*) Regional changes in [18F]dopa metabolism in the striatum in Parkinson's disease. *Brain* 119:2097–103

Naudon L, Leroux-Nicollet I, Costentin J (1994) Short-term treatments with haloperidol or bromocryptine do not alter the density of the monoamine vesicular transporter. *Neurosci Lett* 173:1–4

Niznik HB, Fogel EF, Fassos F, Seeman P (1991) The dopamine transporter is absent in parkinsonian putamen and reduced in the caudate nucleus. *J Neurochem* 56:192–8

Ollinger JM, Johns GC (1993) Model-based scatter correction for fully 3D PET. *IEEE Med Imag Conf Rec* 2:1264–8

Ollinger JM (1995) Detector efficiency and Compton scatter in fully 3D PET. *IEEE Trans Nucl Sci* 42:1168–75

Parkinson Study Group (2002) Dopamine transporter brain imaging to assess the effects of pramipexole versus levodopa on Parkinson disease progression. *JAMA* 287:1653–61

Parkinson Study Group (2004) Levodopa and the rate of progression of Parkinson disease, the ELLDOPA study. *N Engl J Med* 351:2498–508

Peppard RF, Martin WR, Carr GD, Grochowsky E, Schulzer M, Guttman M *et al* (1992) Cerebral glucose metabolism in Parkinson's disease with and without dementia. *Arch Neurol* 49:1262–8

Piert M, Koeppe RA, Giordani B *et al* (1996) Determination of regional rate constants from dynamic FDG-PET studies in Parkinson's disease. *J Nucl Med* 37:1115–22

Pirker W (2003) Correlation of dopamine transporter imaging with parkinsonian motor handicap: how close is it? *Mov Dis* 18(Suppl 7):S43–51

Pristupa ZB, McConkey F, Liu F, Man HY, Lee FJ, Wang YT *et al* (1998) Protein kinase-mediated bidirectional trafficking and functional regulation of the human dopamine transporter. *Synapse* 30:79–87

Reith ME, Xu C, Chen NH (1997) Pharmacology and regulation of the neuronal dopamine transporter. *Eur J Pharmacol* 324:1–10

Sawle GV, Playford ED, Burn DJ *et al* (1994) Separating Parkinson's disease from normality. *Arch Neurol* 51:237–43

Scherman D, Desnos C, Darchen F, Pollak P, Javoy-Agid F, Agid Y (1989) Striatal dopamine deficiency in Parkinson's disease: role of aging. *Ann Neurol* 26:551–7

Scherman D, Raisman R, Ploska A, Agid Y (1988) [3H]dihydrotetrabenazine, a new *in vitro* monoaminergic probe for human brain. *J Neurochem* 50:1131–6

Schulz JB, Skalej M, Wedekind D, Luft AR, Abele M, Voigt K *et al* (1999) Magnetic resonance imaging-based volumetry differentiates idiopathic parkinson's syndrome from multiple system atrophy and progressive supranuclear palsy. *Ann Neurol* 45:65–74

Schwab RS, England AC (1969) Projection technique for evaluating surgery in Parkinson's disease. In: *Third symposium on parkinson's disease* (Gillingham FJ, Donaldson IML, eds), Edinburgh: Livingstone, 152–7

Seibyl JP, Marek KL, Quinlan D, Sheff K, Zoghbi S, Zea-Ponce Y *et al* (1995) Decreased single-photon emission computed tomographic [123I]β-CIT striatal uptake correlates with symptom severity in Parkinson's disease. *Ann Neurol* 38:589–98

Summerfield C, Junque C, Tolosa E, Salgado-Pineda P, Gomez-Anson B, Marti MJ *et al* (2005) Structural brain changes in Parkinson disease with dementia. *Arch Neurol* 62:281–5

Talairach J, Tournoux P (1988) *Co-planar stereotaxic atlas of the human brain*. New York: Thieme

Tedroff J, Ekesbo A, Rydin E, Langstrom B, Hagberg G (1999) Regulation of dopaminergic activity in early Parkinson's disease. *Ann Neurol* 46:359–65

Truong JG, Rau KS, Hanson GR, Fleckenstein AE (2003) Pramipexole increases vesicular dopamine intake: implications for treatment of Parkinson's neurodegeneration. *Eur J Pharmacol* 474:223–6

Ugarte YV, Rau KS, Riddle EL, Hanson GR, Fleckenstein AE (2003) Methamphetamine rapidly decreases mouse vesicular dopamine intake: role of hypothermia and dopamine D2 receptors. *Eur J Pharmacol* 472:165–71

van Dyck CH, Seibyl JP, Malison RT *et al* (1995) Age-related decline in striatal dopamine transporter binding with iodine-123-β-CIT SPECT. *J Nucl Med* 36:1175–81

Vander Borght T, Kilbourn M, Desmond T, Kuhl D, Frey K (1995*b*) The vesicular monoamine transporter is not regulated by dopaminergic drug treatments. *Eur J Pharmacol* 294:577–83

Vander Borght T, Minoshima S, Giordani B, Foster NL, Frey KA, Berent S *et al* (1997) Cerebral metabolic differences in Parkinson's and Alzheimer's diseases matched for dementia severity. *J Nuc Med* 38:797–802

Vander Borght TM, Sima AAF, Kilbourn MR, Desmond TJ, Kuhl DE, Frey KA (1995*a*) [^{3}H]methoxytetrabenazine: a high specific activity ligand for estimating monoaminergic neuronal integrity. *Neuroscience* 68:955–62

Vilpoux C, Leroux-Nicollet I, Naudon L, Raisman-Vozari R, Costention J (2000) Reserpine or chronic paroxetine treatments do not modify the vesicular monoamine transporter 2 expression in serotonin-containing regions of the rat brain. *Neuropharmacol* 39:1075–82

Vingerhoets FJG, Schulzer M, Calne DB, Snow BJ (1997) Which clinical sign of Parkinson's disease best reflects the nigrostriatal lesion? *Ann Neurol* 41:58–64

Volkow ND, Fowler JS, Wang GJ *et al* (1994) Deceased dopamine transporters with age in healthy human subjects. *Ann Neurol* 36:237–9

Weiner HL, Hashim A, Lajtha A, Sershen H (1989) Chronic L-deprenyl-induced up-regulation of the dopamine uptake carrier. *Eur J Pharmacol* 163:191–4

Whone AL, Watts RL, Stoessl AJ, Davis M, Reske S, Nahmias C *et al* (2003) Slower progression of Parkinson's disease with ropinirole versus levodopa: the REAL-PET study. *Ann Neurol* 54:93–101

Wilson JM, Kish SJ (1996*a*) The vesicular monoamine transporter, in contrast to the dopamine transporter, is not altered by chronic cocaine self-administration in the rat. *J Neurosci* 16:3507–10

Wilson JM, Levey AI, Rajput A, Ang L, Guttman M, Shannak K *et al* (1996*b*) Differential changes in neurochemical markers of striatal dopamine nerve terminals in idiopathic Parkinson's disease. *Neurology* 47:718–26

Wilson JM, Nobrega JN, Carroll ME *et al* (1994) Heterogeneous subregional binding patterns of ^{3}H-WIN35,428 and ^{3}H-GBR12,935 are differentially regulated by chronic cocaine self-administration. *J Neurosci* 14: 2966–29

Young EA, Neff NH, Hadjiconstantinou M (1993) Evidence for cyclic AMP-mediated increase of aromatic L-amino acid decarboxylase activity in the striatum and midbrain. *J Neurochem* 60:2331–3

Zelnik N, Angel I, Paul SM, Kleinman JE (1986) Decreased density of human striatal dopamine uptake sites with age. *Eur J Pharmacol* 126:175–6

Zhu M-Y, Jucrio AV, Paterson IA, Boulton AA (1993) Regulation of striatal aromatic amino acid decarboxylase: effects of blockade or activation of dopamine receptors. *Eur J Pharmacol* 238:157–64

Zhu SJ, Kavanaugh MP, Sonders MS, Amara SG, Zahniser NR (1997) Activation of protein kinase C inhibits uptake, currents and binding associated with the human dopamine transporter expressed in *Xenopus* oocytes. *J Pharmacol Exp Ther* 282: 1358–1365

Zubieta JK, Huguelet P, Ohl LE, Koeppe RA, Kilbourn MR, Carr JM *et al* (2000) High vesicular monoamine transporter binding in asymptomatic bipolar I disorder: sex differences and cognitive correlates. *Am J Psychiatry* 157:1619–28

Zucker M, Weizman A, Harel D, Rehavi M (2001) Changes in vesicular monoamine transporter (VMAT2) and synaptophysin in rat substantia nigra and prefrontal cortex induced by psychotropic drugs. *Neuropsychobiology* 44:187–91